Forced lipid catabolism entails higher proliferation rate of cervical cancer cells by ROS-dependent HIF1α activation

Serena Castelli[1], Fabio Ciccarone[2], Daniela Tavian[3], Maria Rosa Ciriolo[1,4]

[1] Department of Biology, University of Rome "Tor Vergata", Via della Ricerca Scientifica 1, Rome 00133, Italy;
[2] IRCCS San Raffaele Pisana, Department of Human Sciences and Promotion of the Quality of Life, San Raffaele Roma Open University, Rome, Italy.
[3] Laboratory of Cellular Biochemistry and Molecular Biology, CRIBENS, Catholic University of the Sacred Heart, pz Buonarroti 30, 20145 Milan, Italy.
[4] IRCCS San Raffaele Pisana, Via della Pisana 235, Rome 00163, Italy

Abstract

The high proliferative capacity of cancer cells is responsible for higher energy and building blocks molecules demand, which require a metabolic reprogramming. Metabolic rewiring of cancer cells, usually, involves a switch towards aerobic glycolysis for a rapid energy supply, a phenomenon known as the "Warburg effect". Moreover, lipid metabolism derangement is also essential due to the several intracellular functions of lipids: i) ignition of oxidative energy production; ii) source for membrane biogenesis; iii) second messengers; and iv) post-translational modification of proteins. Based on this knowledge, one of the most promising interventions in cancer therapy to specifically inhibit cancer cell survival is to affect cell metabolism. While the aerobic glycolytic pathway was the first to be targeted, most recent approaches are dealing with the contribution of lipid metabolism in the malignancy of cancer cells. Boosting lipid catabolism was obtained by over-expressing of the adipose triglyceride lipase (ATGL), the first and rate-limiting enzyme of lipolysis in the cervical cancer cell line HeLa. ATGL catalytic mutant and caproate, a short-chain fatty acid that is efficiently oxidized in mitochondria, were exploited to associate the observed effects with the lipolytic activity of ATGL. Here, we highlight the association between boosted lipid catabolism and the increased proliferation and migration capability of HeLa cells. The reactive oxygen species (ROS), produced by the increased mitochondrial fatty acids (FAs) oxidation, mediated these pro-tumoral effects by triggering hypoxia-inducible factor-1α (HIF1α). HIF1α doubly promoted the aggressive phenotype: on one hand, by increasing glycolytic flux and lactate production; on the other hand, by inducing its known target BCL2 and adenovirus E1B 19-kDa-interacting protein 3 (BNIP3). In turn, BNIP3 promoted cell survival by activating mitophagy as a mechanism to scavenge ROS. Indeed, upon inhibition of mitophagy, we observed the induction of apoptosis. The phenotype is recapitulated by the short-chain fatty acid caproate, confirming that forcing lipid catabolism resulted in HIF1α induction. Our findings highlight a correlation between ATGL activity and the aggressiveness of cervical cancer cells, suggesting that ATGL could be a promising prognostic marker for cervical cancer.

Results

1. Boosting lipid catabolism is associated with the higher aggressiveness of cervical cancer cells

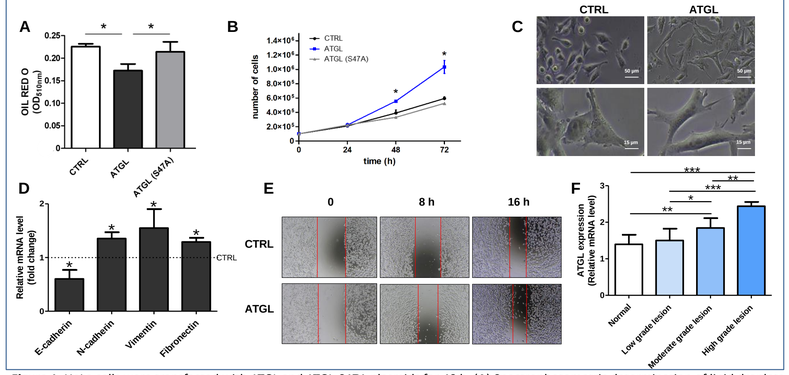

Figure 1. HeLa cells were transfected with ATGL and ATGL-S47A plasmids for 48 h. (**A**) Spectrophotometric determination of lipid droplets content after OIL red O staining. Relative absorbance was normalized on total proteins. Data are expressed as mean ± SD (n=3; * *p<0.05* as indicated). (**B**) Proliferation was assayed by Trypan blue direct cell counting procedure. Data are expressed as mean ± SD (n=3; * *p<0.05 vs.* CTRL and ATGL-S47A). (**C**) Morphological change of HeLa cells transfected with pcDNA™4/HisMaxC and pcDNA™4/HisMaxC-ATGL for 48 h. (**D**) RT-qPCR analysis of E-cadherin, N-cadherin, Vimentin and Fibronectin mRNA. β-Actin (*ACTB*) was used as reference control. Data are shown as fold change *vs.* CTRL represented by a dashed line in the bar graph (n=4; * p<0.05 *vs.* CTRL). (**E**) Wound Healing assay. Images, representative of three independent experiments, were taken at 0, 8, and 16 h from "wound" formation. (**F**) *Patatin Like Phospholipase Domain Containing 2* (*PNPLA2)* gene expression in different grade of cervical cancer was assessed by Gene Expression Omnibus (GEO; http://www.ncbi.nlm.nih.gov/geo, accession number GSE63514) through an Affymetrix Human Genome Array (100 samples of cervical cancer subdivided for grade *vs.* normal cervical epithelium) (* *p<0.05;* ** *p<0.01;* *** *p<0.001* as indicated).

2. ATGL over-expression promotes "Warburg effect" in HeLa cells

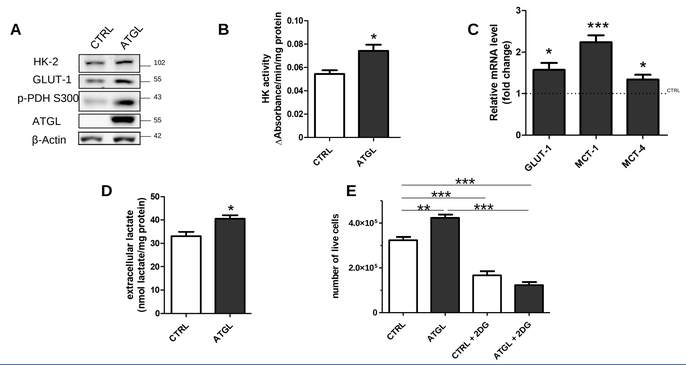

Figure 2. HeLa cells were over-expressed for 48 h and glycolytic metabolism was monitored by: (**A**) Western blot analysis of hexokinase-2 (HK-2), glucose transporter-1 (GLUT-1) and phosphorylated pyruvate dehydrogenase (p-PDHE1α S300) levels. The images are representative of three independent experiments that gave similar results. β-Actin and ATGL were used as loading and transfection control, respectively; (**B**) spectrophotometric determination of hexokinase (HK) activity. Relative absorbance was normalized on total proteins and data are expressed as mean ± SD (n=3; * p<0.05 vs. CTRL); (**C**) the expression levels of glucose and lactate transporters genes through RT-qPCR analysis of GLUT1, MCT1 and MCT4. ACTB was used as reference control. Data are shown as fold change vs. CTRL represented by a dashed line in the bar graph (n=3; * p<0.05 vs. CTRL); (**D**) Evaluation of extracellular lactate content was performed on cell culture media collected after 48 h of ATGL over-expression. Relative absorbance was normalized on total proteins and data are expressed as mean ± SD (n=3; * p<0.05 vs. CTRL). Cells were treated with the glycolysis inhibitor 2-deoxyglucose (2DG, 10 mM) 24 h before the end of the experiment upon ATGL over-expression and (**E**) proliferation rate was assayed by Trypan blue direct cell counting procedure. Data are expressed as mean ± SD (n=3; ** p<0.01; *** p<0.001 as indicated).

3. BNIP3-mediated mitophagy becomes a pro-survival mechanism to scavenge ROS derived from ATGL activity

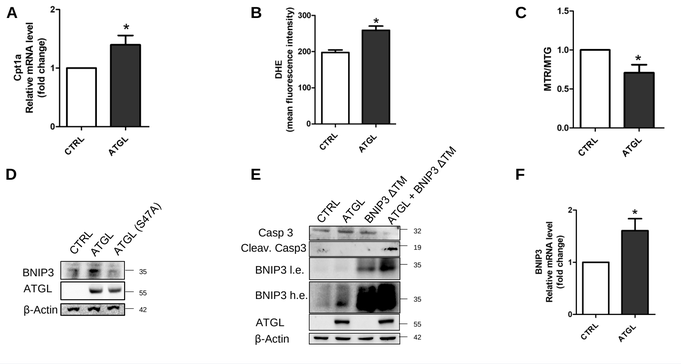

Figure 3. HeLa cells were over-expressed for 48 h and (**A**) RT-qPCR analysis of Cpt1a mRNA. ACTB was used as reference control. Data are showed as fold change vs. CTRL (n=3; * p<0.05 vs. CTRL). (**B**) Reactive Oxygen Species (ROS) were quantified by cytofluorimetric analysis. Cells were treated with 50 μM of DHE 30 min before the end of the experiment. 10 000 events were counted. Data are expressed as mean ± SD (n=3; * p<0.05 vs. CTRL). (**C**) Ratio between the mean fluorescence intensity of MTR and of MTG. Cytofluorimetric analysis was performed after treatment with 200 μM of MTR and MTG 30 min before the end of the experiments. 10 000 events were counted. Data are expressed as mean ± SD (n=3; * p<0.05 vs. CTRL). (**D**) After over-expression of ATGL and ATGL-S47A (catalytic mutant), BNIP3 levels were evaluated by Western blot analysis. β-Actin and ATGL were used as loading and transfection control, respectively. HeLa cells were transfected with pATGL and BNIP3 ΔTM (dominant negative mutant) plasmid for 48 h and (**E**) Western blot analysis of cleaved caspase 3 was assayed. Images are representative of three independent experiments that gave similar results. β-Actin was used as loading and transfection control; ATGL and BNIP3 were used as transfection controls. (**F**) RT-qPCR analysis of BNIP3 mRNA. ACTB was used as reference control. Data are showed as fold change vs. CTRL (n=3; * p<0.05 vs. CTRL).

4. ATGL activity induces transcriptionally HIF1α in a ROS-dependent fashion

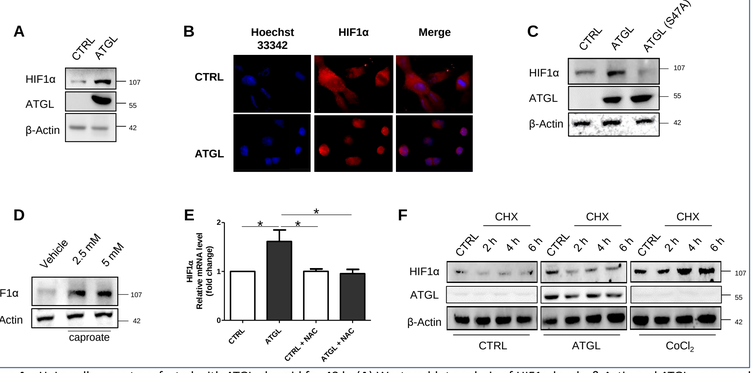

Figure 4. . HeLa cells were transfected with ATGL plasmid for 48 h. (**A**) Western blot analysis of HIF1α levels. β-Actin and ATGL were used as loading and transfection control, respectively. Images are representative of six independent experiments that gave similar results. (**B**) Immunofluorescent analysis of HIF1α subcellular localization in HeLa cells after ATGL over-expression. Images are representative of three independent experiments that gave similar results. Nuclei were stained 10 min with 1 μg/mL Hoechst 33342. (**C**) After over-expression of ATGL and ATGL-S47A, HIF1α levels were evaluated by Western blot analysis. Images are representative of three independent experiments that gave similar results. β-Actin and ATGL were used as loading and transfection control, respectively. (**D**) Western blot analysis of HIF1α levels performed for HeLa cells treated with 2.5 mM and 5 mM caproate, that mimics ATGL activity, for 24 h. Images are representative of three independent experiments that gave similar results. β-Actin was used as loading control. (**E**) RT-qPCR analysis of HIF1α levels was performed. ACTB was used as reference control. Data are shown as fold change (n=3; * p<0.05 as indicated). (**F**) Cells were treated with Cycloheximide (CHX, 10 μg/mL) for 2, 4, 6 h and cobalt chloride (CoCl2, 150 μM) for 6 h before the end of experiment and HIF1α protein levels were evaluated by Western blot analysis. The images are representative of three independent experiments that gave similar results. β-Actin and ATGL were used as loading and transfection control, respectively.

5. HIF1α is responsible for BNIP3 induction and "Warburg effect" rise

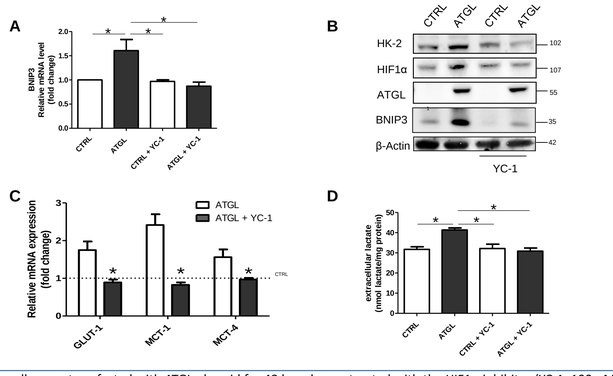

Figure 5. . HeLa cells were transfected with ATGL plasmid for 48 h and were treated with the HIF1α inhibitor (YC-1, 100 μM) 24 h before the end of the experiment.(**A**) RT-qPCR analysis of BNIP3 mRNA was performed. ACTB was used as reference control. Data are shown as fold change (n=3; * p<0.05 as indicated). Glycolytic metabolism was monitored by: (**B**) Western blot analysis of HK-2 levels. β-Actin and ATGL were used as loading and transfection control, respectively; HIF1α was evaluated as YC-1 treatment control. Images are representative of three independent experiments that gave similar results; by (**C**) RT-qPCR analysis of GLUT1, MCT1 and MCT4 mRNA. ACTB was used as reference control. Data are shown as fold change (n=3; * p <0.05 vs ATGL). CTRL was represented by a dashed line in the bar graph. (**D**) Evaluation of extracellular lactate content, relative absorbance was normalized on total proteins. Data are expressed as mean ± SD (n=3; * p<0.05; ** p<0.01 as indicated)

6. ROS are upstream mediators of ATGL activity in HeLa cells

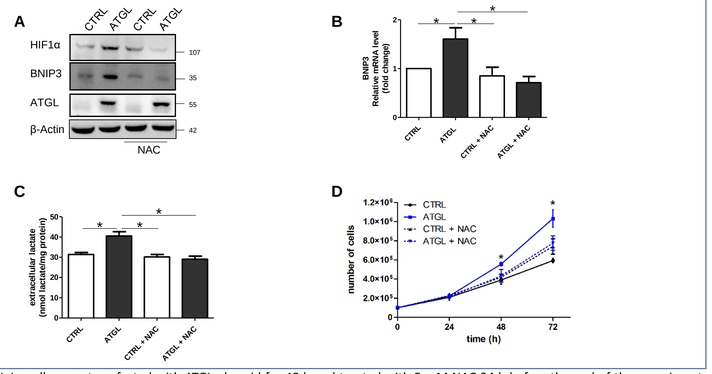

Figure 6. . HeLa cells were transfected with ATGL plasmid for 48 h and treated with 5 mM NAC 24 h before the end of the experiment. (**A**) HIF1α and BNIP3 levels were analyzed by Western blot analysis. The images are representative of three independent experiments that gave similar results. β-Actin and ATGL were used as loading and transfection control, respectively. (**B**) RT-qPCR analysis of BNIP3 levels. ACTB was used as reference control. Data are shown as fold change (n=3; * p<0.05 as indicated). (**C**) The evaluation of extracellular lactate content was performed on cell culture media collected after 48 h of ATGL over-expression by spectrophotometric analysis. Data are expressed as mean ± SD (n=3; * p<0.05 as indicated). (**D**) The proliferation was assayed by Trypan blue direct cell counting procedure. Data are expressed as mean ± SD (n=3; * p<0.05 vs. ATGL + NAC).

Conclusions

Overall, we propose a pro-tumor role of ATGL that is dependent on ROS which could be exploited for creating new personalized therapy based on the specific antioxidant system of tumor cells. Interestingly, ROS deriving from ATGL activity activate HIF1α, which represents a key orchestrator of radioresistance and paclitaxel resistance of cervical cancer. Despite these therapeutic approaches have different mechanisms of action, they all lead to an increase in ROS production. For this reason, the link here described between ATGL and HIF1α signaling mediated by ROS exposes a potential intervention point aimed to restrain cell resistance of cervical cancer cells.

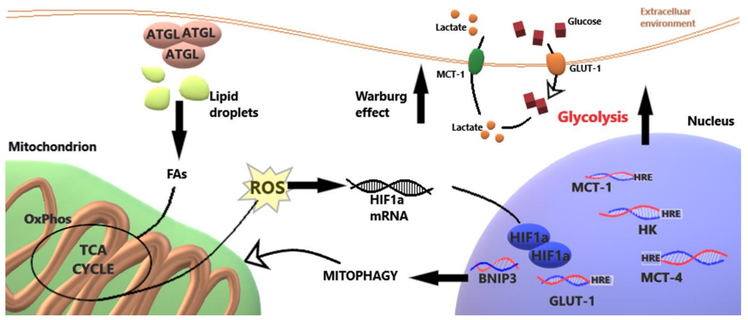

Contact

Serena Castelli
serenacastelli93@gmail.com
+39 06 7259 4360

Prof. Maria Rosa Ciriolo
ciriolo@bio.uniroma2.it
+39 06 7259 4369

Fabio Ciccarone
fabio.ciccarone83@gmail.com
+39 06 72594360